# Grafting of Cross-Linked Hydrogel Networks to Titanium Surfaces

Beinn V. O. Muir,[¶,‡,†] David Myung,[¶,‡] Wolfgang Knoll,[¶,§,∥] and Curtis W. Frank*,[¶]

[¶]Department of Chemical Engineering, Stanford University, 381 North-South Mall, Stauffer III, Stanford, California 94305-5025, United States

[§]Materials Science, Max Planck Institute for Polymer Research, Ackermannweg 10, Mainz, Rhineland-Palatinate 55128, Germany

**ABSTRACT:** The performance of medical implants and devices is dependent on the biocompatibility of the interfacial region between tissue and the implant material. Polymeric hydrogels are attractive materials for use as biocompatible surface coatings for metal implants. In such systems, a factor that is critically important for the longevity of an implant is the formation of a robust bond between the hydrogel layer and the implant metal surface and the ability for this assembly to withstand physiological conditions. Here, we describe the grafting of cross-linked hydrogel networks to titanium surfaces using grit-blasting and subsequent chemical functionalization using a silane-based adhesion promoter. Metal surface characterization was carried out using profilometry, scanning electron microscopy (SEM), and energy dispersive X-ray spectroscopy (EDX) analysis. Hydrogel layers composed of poly(ethylene glycol)-dimethacrylate (PEG-DMA), poly(2-hydroxyethylmethacrylate) (PHEMA), or poly(ethylene glycol)/poly(acrylic acid) (PEG/PAA) semi-interpenetrating polymer networks (semi-IPNs) have been prepared. The mechanical properties of these hydrogel-metal assemblies have been characterized using lap-shear measurements, and the surface morphology was studied by SEM and EDX. We have shown that both high surface roughness and chemical functionalization are critical for adhesion of the hydrogel layer to the titanium substrate.

**KEYWORDS:** hydrogel grafting, cross-linked networks, medical implants, semi-interpenetrating networks, tribochemical modification, grit-blasting, titanium, lap-shear adhesion
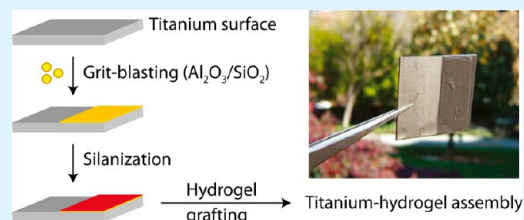
## INTRODUCTION

The performance of many biomedical implants and devices is dependent on the surface characteristics of the implant material. Hydrogel coatings are now being developed and used by investigators extensively to lower the thrombogenicity and immunogenicity of implanted devices,[1−3] phenomena that are usually initiated by the adsorption of body fluid proteins on the implant. Improvement of tribological properties is also important in orthopedic devices, almost all of which involve sliding articulations between two implant surfaces, and cross-linked hydrogels have been demonstrated as low friction coatings.[4] In many dental implants and total joint prostheses, the implanted device requires the attachment of a metallic component, usually composed of titanium or titanium alloys,[5,6] to bone. Thus, the bulk and surface character of the device material are of critical importance to their success.[7,8] Tethering hydrogels to implanted materials may provide a route to improve the biocompatibility and overall performance of these devices.

Various researchers have modified titanium surfaces for biomedical applications in order to increase biocompatibility. Thermo-chemical treatment has been shown to reduce corrosion and improve fatigue lifetime of titanium and titanium alloys.[9,10] Treatment of titanium with ultraviolet light, known as UV-photofunctionalization, improved adhesion of osteoblast cells to titanium[11,12] and accelerated bone integration of titanium implants.[13] Improved biocompatibility of titanium implants has been shown using a variety of coatings including glass,[14] diamond-like carbon,[15] hydroxyapatite/titania sol—gel,[16] and chitosan.[17] Hydrogel layers offer another route toward biocompatibility, and hydrogels have been prepared on mineral surfaces using a variety of techniques, including electrochemistry,[18,19] layer-by-layer growth,[20] and photochemical attachment.[21,22] In particular, Rühe and co-workers have extensively studied photochemical attachment and cross-linking of polymer layers on a variety of substrates using different linkers including benzophenone,[23−25] α-diazoester,[26] and sulfonyl azide groups.[27]

While hydrogels have been prepared on a variety of surfaces, obtaining robust adhesion of hydrogels for high stress applications has been a challenge. In this work, we apply a tribochemical strategy adapted from dentistry[28,29] that provides strong adhesion between metals and polymers in the dental industry to the adhesion of water swollen hydrogel layers to the surface of titanium.[30] Previously, Matinlinna et al.[28] described the bonding of the dental resin *bis*-phenol A diglycidyldimethacrylate (bis-GMA) to grit-blasted titanium through the use of isocyanato- and methacryloxysilanes. The hydrogel bonding process described in our work involves an initial grit-blasting step in which a layer of $SiO_2$ is embedded within the surface of titanium,[31−33] followed by coupling of a molecule containing a photoreactive functional group to the $SiO_2$ by silane

chemistry[34] and finally grafting of the hydrogel to the surface by photopolymerization. Depending on the nature of the hydrogel grafted to the surface, these hydrogel-titanium assemblies may be used in a variety of biomedical device applications that require a robust hydrophilic surface layer.

In this paper, we use a variety of analytical techniques to study the hydrogel-metal interface. Profilometry was used to compare the roughness of grit-blasted and unmodified surfaces, while contact angle measurements were used to confirm chemical modification of the silanized surfaces. Pairs of surfaces possessing identical treatments were bonded together via the photopolymerization of a hydrogel precursor solution consisting of either poly(ethylene glycol)-dimethacrylate (PEG-DMA) or poly(2-hydroxyethylmethacrylate) (PHEMA), through the formation of single networks, or a semi-interpenetrating polymer network (semi-IPN) of poly(ethylene glycol)-diacrylate (PEG-DA) and linear poly(acrylic acid) (PEG/PAA network). The grafted hydrogel layer acted as the "adhesive" between the two metal plates. Lap-shear adhesion testing and swelling experiments were carried out on each hydrogel-metal assembly to determine the robustness of the hydrogel-titanium bond. Scanning electron microscopy (SEM) and energy dispersive X-ray spectroscopy (EDX) with composition mapping were carried out on the fractured interfaces of the shear-tested hydrogel-titanium assemblies.

## ■ EXPERIMENTAL SECTION

**Materials.** Titanium plates (99% pure), each with an area of 6.5 cm$^2$ and a thickness of 1 mm, were obtained from Alfa Aesar (Ward Hill, MA). In this paper, PEG macromonomers will be distinguished on the basis of their molecular weight using the following nomenclature: PEG macromonomers with molecular weight $X$ Daltons will be designated PEG($X$). PEG(1000)-dimethacrylate was obtained from Polysciences (Warrington, PA), while PEG(4600), 2-hydroxyethylmethacrylate (HEMA), poly(acrylic acid) (PAA, MW 250,000), anhydrous tetrahydrofuran, acryloyl chloride, and 2-hydroxy-2-methyl-propiophenone were obtained from Sigma-Aldrich (St. Louis, MO). 3-(Trimethoxysilyl)propyl methacrylate (TMSPM) (3 M ESPE "Sil" reagent) was used for silane coupling and was obtained from 3 M (St. Paul, MN). The Rocatec Jr. Blasting module and SiO$_2$-coated alumina sand particles were obtained from 3 M (St. Paul, MN).

**Methods.** *Titanium Modification.* Titanium samples were manually grit-blasted using the Rocatec Junior Bonding system. The titanium surfaces were grit-blasted with SiO$_2$-coated alumina particles (~110 $\mu$m in diameter) at a pressure of 2.8 bar for five seconds per square millimeter with the nozzle positioned perpendicular to and 1 cm away from the titanium surface. A high level of energy is created by the acceleration of the particles to a velocity of up to 1000 km/h within the blast nozzle.[35] Modification of the blasted surface takes place when the grains hit the surface creating a so-called "triboplasma" and SiO$_2$ is impregnated into the surface up to a depth of 15 $\mu$m, as described by the manufacturer.[35] The particles are fused to the surface in islands, as shown in Figures 5 and 6. Apart from "ceramicizing" the surface of titanium, the impact of the particles also causes a certain amount of roughening, as characterized using profilometry. To serve as a basis for comparison for the grit-blasted surfaces, titanium was also modified with a continuous SiO$_2$ layer by a vapor deposition process to yield coated surfaces that were not roughened. The silicon dioxide film was deposited on piranha cleaned titanium using a low temperature plasma enhanced chemical vapor deposition (PECVD) system (Surface Technology Systems (STS) plc, Newport, UK), at a deposition rate of 35 nm/min, carried out in high frequency mode at 40 W, 650 mTorr, and 350 °C, using 2% silane (in argon carrier gas) and nitrous oxide as precursors. (*Caution: "Piranha" solution reacts violently with organic materials; it must be handled with extreme care.*) Film thickness, based on deposition on a piranha-cleaned standard

⟨100⟩ silicon wafer, was determined to be 114 nm using single wavelength fixed angle ellipsometry on a Rudolph Research AutoEL III Ellipsometer (Rudolph Technologies Inc., New Jersey, USA) equipped with a 632.8 nm HeNe 0.2 mW class II laser set at an angle of 70°. The refractive index of the film was determined to be 1.47.

*Silane Coupling to Ceramicized Titanium.* The SiO$_2$-coated titanium was chemically functionalized by drop-casting a solution of Sil Reagent (3 M) containing 3-(trimethoxysilyl)propyl methacrylate (TMSPM), a heterobifunctional linker, in ethanol and water onto its surface, allowing the solvent to evaporate and the linker to react for five minutes. This creates a linkage between the silane group and the SiO$_2$ surface, leaving the methacrylate groups free to react with other methacrylate or acrylate-containing monomers or macromonomers.

*Hydrogel Precursor Solution Preparation.* PEG-DMA networks were synthesized from a 50% by weight solution of PEG(1000)-DMA in deionized water along with 1% v/v (with respect to the macromonomer) 2-hydroxy-2-methyl-propiophenone as the photoinitiator. PHEMA single networks were synthesized from a 65% v/v aqueous solution of 2-hydroxyethylmethacrylate (Sigma-Aldrich, St. Louis, MO) containing 1% v/v (with respect to the monomer) 2-hydroxy-2-methyl-propiophenone as the photoinitiator. PEG/PAA semi-interpenetrating polymer networks were prepared as follows. First, PEG(4600)-DA was synthesized by first dissolving the PEG(4600) macromonomer in anhydrous tetrahydrofuran at 50 °C. Next, a molar excess of acryloyl chloride was added to the PEG solution and allowed to react for 5 h under a nitrogen atmosphere. The solution was allowed to cool to room temperature and then was precipitated at 4 °C. The PEG-DA was then purified by reprecipitation in fresh anhydrous tetrahydrofuran. Purified PEG-DA was then dissolved in deionized water along with 5% by volume linear poly(acrylic acid). The water-soluble photoinitiator, 2-hydroxy-2-methyl propiophenone, was then added to the PEG-DA solution at a concentration of 1% by weight with respect to the macromonomer.

*Bonding of Hydrogels to Titanium.* In these experiments, PEG(1000) single networks, PEG/PAA semi-interpenetrating networks, or PHEMA single networks were bonded to titanium plates. The tribochemical process used for bonding the hydrogel and titanium components proceeded as follows: (1) a layer of SiO$_2$ was embedded within the titanium surface by grit-blasting with SiO$_2$-coated alumina particles, (2) the heterobifunctional coupling agent 3-(trimethoxysilyl)propyl methacrylate was deposited on the surface and reacted with the SiO$_2$ to form Si−O−Si bonds on the surface of the SiO$_2$, and (3) acrylate and/or methacrylate-containing monomers and/or macromonomers were cast over and copolymerized with the methacrylate groups on the SiO$_2$-coated titanium by UV-initiated free radical polymerization using a 365 nm UV light operating at 30 mW/cm$^2$ (Electro-lite, Inc.) on a rotating stage for 10 min.

*Profilometry.* Surface characterization was carried out using a Dektak 150 Surface Profiler (Veeco Instruments Inc., Tucson, AZ) using a B-type (red) stylus with a 12.5 $\mu$m tip diameter. Two-dimensional profiles were measured using a 2 mm scan length with a duration of 60 s (33 $\mu$m/s), resulting in a resolution of 111 nm/sample. The binning range was set to 65.5 $\mu$m with a stylus force of 10 mg (as recommended by the manufacturer for hard surfaces). All samples were leveled (to remove sample tilt) before roughness calculation using Dektak V9 Software.

*Contact Angle.* Measurements were taken using a FTÅ200 contact angle apparatus with a motorized syringe pump (First Ten Ångstroms, Portsmouth, VA). Image capture used a Sanyo camera with supplied FTÅ200 video software V1.98 (AccuSoft Corp., Northborough, MA). Standard drop size was 6 $\mu$L (syringe operating at 0.3 $\mu$L/s and ~20 s per drop).

*Scanning Electron Microscopy (SEM).* For SEM, all samples were briefly washed with ethanol, dried with a stream of nitrogen gas, and mounted onto Al stubs using Electrodag 502 (Ted Pella, Inc., Redding, CA) conductive carbon adhesive. Samples were then sputter coated using a Cressington 108auto DC magnetron sputter coater with planetary motion tilting rotary stage (Watford, England), with a 1−2 nm Au$_{60}$Pd$_{40}$ alloy, at a current of 20 mA for 45 s under a low pressure (0.08 mbar) Ar atmosphere. This coating was applied in order to

959

dx.doi.org/10.1021/am404361v | *ACS Appl. Mater. Interfaces* 2014, 6, 958−966

increase surface electrical conductivity and improve imaging resolution and image stability. Scanning electron microscopy was carried out using a FEI XL Sirion SEM (FEI Company, Hillsboro, OR) having a FEG source operating at an acceleration voltage of 5 kV, with spot size 3, under high vacuum. Low magnification images (100−10 000×) were collected using a standard secondary electron (SE) detector. High magnification images (>10 000×) were collected with an in-lens SE detector using through lens detection (TLD) mode. All images are presented as obtained without modification.

*Energy Dispersive X-ray Spectroscopy (EDX).* Energy dispersive X-ray spectroscopy analysis and EDX compositional maps were obtained using an EDAX microanalysis module (EDAX, Mahwah, NJ) at an accelerating voltage of 15 kV. EDX analysis was carried out concurrently and on the same samples as SEM analysis. Each compositional map consists of approximately 100 frames using a dwell time of 200 $\mu$s and was collected using EDAX Genesis analysis software V4.61.

*Lap-Shear Adhesion.* The strength of the hydrogel-titanium bond was tested using lap-shear adhesion experiments (ASTM D3163) in which the surfaces of two titanium plates were bonded together using a 250 $\mu$m thick hydrogel layer and pulled apart with a motion parallel to the surfaces using an Instron 5844 materials testing apparatus equipped with a 1 kN load cell (Instron Corp, Norwood, MA). The effect of grit-blasting and/or silane functionalization of the titanium surfaces on hydrogel adhesion was tested. In addition, three different hydrogels were tested: (1) a PEG(1000)-DMA macromonomer, (2) a cross-linked PHEMA single network, and (3) a PEG/PAA semi-interpenetrating network using PEG(4600)-DA, all of which would be expected to form bonds with the methacrylate groups on the chemically functionalized titanium surface. The aforementioned hydrogel precursor solutions were each injected between staggered titanium plates that were previously grit-blasted and/or silane-treated, separated by 250 $\mu$m-thick Teflon spacers (Goodfellow Corp, Coraopolis, PA), and then exposed to 365 nm UV radiation for 10 min. The staggered, adherent plates were soaked in deionized water overnight prior to testing. The lap-shear experiments involved gripping the free end of the titanium plates and then pulling them in opposite directions, while collecting both load and extension data.

## RESULTS

**Hydrogel Grafting.** The chemical reaction in which the telechelic PEG macromonomers are attached to titanium surfaces is shown in Figure 1. In the presence of methacrylate-functionalized PEG macromonomers, two types of chemical linkages can be made: (1) between the surface linker and the PEG macromonomer (dotted ellipses) and (2) between PEG macromonomers (arrows). In this way, hydrogels were chemically bonded to the surface of titanium plates.

**Hydrogel Network Formation.** Single network hydrogels based on a monomeric precursor were prepared on various titanium surfaces. This process is illustrated in Figure 2 for a silane functionalized titanium surface.

In addition, semi-interpenetrating polymer networks of PEG(4600)-DA and PAA were prepared on the titanium surfaces. A neutral telechelic macromonomer network of PEG(4600)-DA was covalently bonded to the surface of the titanium. Interpenetrating this was a physical network of linear PAA polymer chains of 250 000 Da. Schematics showing the synthesis and bonding of this semi-interpenetrating PEG/PAA network to titanium are shown in Figure 3.

**Grit-Blasting of Titanium.** Titanium plates were grit-blasted using SiO$_2$-coated alumina particles. Figure 4 shows profilometry data (values given in Table 1) on the roughness of the grit-blasted titanium, compared with unroughened and untreated titanium and glass that were measured as obtained (samples were cleaned with ethanol prior to analysis to remove
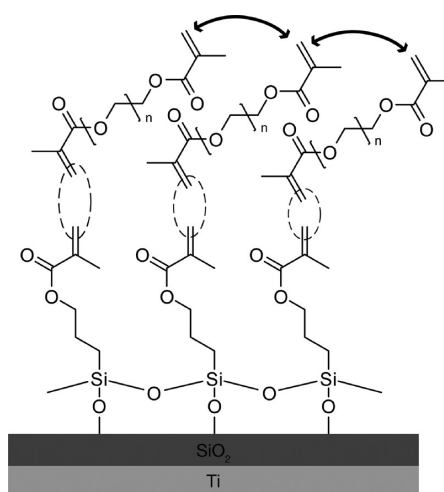


**Figure 1.** The TMSPM molecules tethered to Ti/SiO$_2$ can make further covalent linkages via free-radical polymerization with acrylate-containing molecules (within dotted ellipses), such as poly(ethylene glycol) diacrylate macromonomers (PEG-DMA, top). The PEG-DMA molecules can also be covalently linked with each other (arrows). The TMSPM monolayer structure as shown here is a highly idealized representation, and for clarity, the Ti/SiO$_2$ layers are represented as continuous and uniform films.
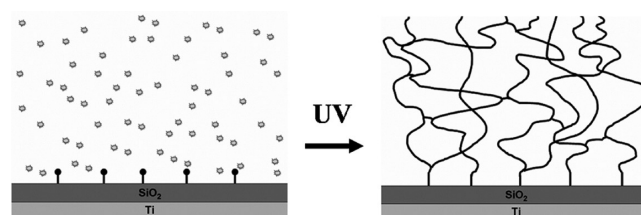


**Figure 2.** To form a monomer-based single network on a titanium surface, acrylate or methacrylate-based monomers (unfilled small circles) are cast over a titanium/SiO$_2$ surface that is functionalized with UV-sensitive cross-linkable groups (filled small circles), along with photoinitiator and a cross-linking agent (not shown). Exposure to UV light in the presence of a photoinitiator leads to free-radical polymerization and cross-linking of the monomers with each other and with the SiO$_2$ surface. The result of the free-radical polymerization and cross-linking is shown on the right. Note that the substrate thicknesses and hydrogel layer dimensions are not to scale.

any oils or debris). The grit-blasted titanium had the highest average roughness (Ra) (over 1700 nm), which was over three times that measured for both the vapor-deposited SiO$_2$ modified titanium and untreated titanium (~500 nm). Untreated glass had a roughness on the order of 6 nm.

Titanium samples were grit-blasted in such a way that 50% of the surface was grit-blasted and the remaining area was left unmodified (unblasted region). SEM analyses of the grit-blasted and unmodified areas (Figure 5a−d) showed that the titanium surfaces that were directly treated were successfully impregnated with SiO$_2$, indicated by grayscale contrast between the grit-blasted region, Figure 5a, left, and unmodified region, Figure 5a, right, where the contrast is due to the build up of electrical charge within the insulating SiO$_2$ layer.

At high magnification (Figure 5c,d), the SEM images show that the SiO$_2$ layer appears as a densely packed, discrete white particulate material. At the same time, some residual particulates appeared to have contaminated the unblasted region, as shown in Figure 5b, presumably due to the
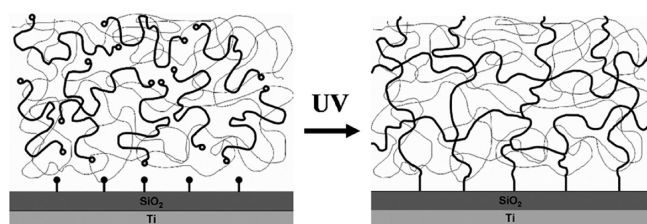
dx.doi.org/10.1021/am404361v | *ACS Appl. Mater. Interfaces* 2014, 6, 958−966

**Figure 3.** To form a semi-interpenetrating network on the surface of titanium, telechelic PEG-DA (dark lines) with UV-sensitive cross-linkable groups (unfilled small circles) and PAA linear polymers (gray lines) are mixed together in solution and cast over a titanium/$SiO_2$ surface that is functionalized with UV-sensitive cross-linkable groups (filled small circles). Exposure to UV light in the presence of a photoinitiator leads to free-radical polymerization and cross-linking of these cross-linkable groups on both the PEG-DA molecules and the $SiO_2$ surface. The result of free-radical polymerization and cross-linking is shown on the right. The ends of the PEG-DA macromonomers (dark lines) have copolymerized and bonded with the surface of the $SiO_2$. The PAA polymers (gray lines) are physically trapped within this first network, forming a second, physically cross-linked network interpenetrating the first chemically cross-linked network.
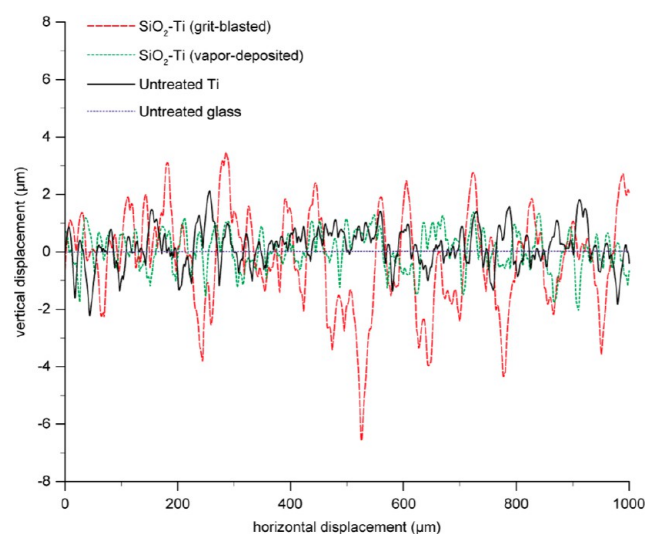


**Figure 4.** Profilometry measurements for untreated and $SiO_2$-coated titanium substrates as well as untreated glass.



**Figure 5.** SEM analysis of partially grit-blasted titanium surface. Part (a) shows both grit-blasted, $SiO_2$-modified (left, lighter), and unmodified (right, darker) regions. The dashed white line is intended to the guide the eyes along the border between the two regions. Part (b) shows a magnified view of the adjacent unmodified titanium region, with inset showing high magnification SEM image of the titanium surface. It can be seen that the grit-blasting process leaves particulates (white) on the adjacent titanium (dark). Parts (c) and (d) show higher magnification SEM images of the grit-blasted area. Scale bars indicate (a) 100 $\mu$m, (b, c) 2 $\mu$m, and (d) and (b, inset) 400 nm.



**Figure 6.** EDX composition map of the interface between the grit-blasted and unmodified regions (a), with the corresponding SEM image shown in (b). The white dashed line is there to aid the eye. (c) EDX analysis of a central area within the grit-blasted region. (d) High magnification EDX composition map of the same area. EDX legend: green, Si; red, Al; blue, Ti. Si rich regions are likely to be in the form of $SiO_2$ and Al rich regions in the form of $Al_2O_3$. Scale bars indicate (a–c) 100 $\mu$m and (d) 2 $\mu$m.

deposition of $SiO_2$ coated alumina particles from "collateral damage" caused by the grit-blasting process. Dark gray regions in Figure 5b are thought to consist of an unmodified titanium surface, with the inset in Figure 5b showing a high magnification SEM image of the unmodified titanium surface structure.

In order to determine the atomic composition of the grit-blasted and unmodified areas, we carried out elemental composition mapping (Figure 6a–d) through energy dispersive X-ray spectroscopy (EDX). The EDX composition maps shown in Figure 6 clearly show that the grit-blasted regions are heterogeneous, with roughly equal distributions of $SiO_2$, $Al_2O_3$, and residual titanium metal.

**Surface Chemistry.** Table 1 summarizes the various surfaces prepared and their average roughness, followed by the post-treatment used (plasma cleaning or no plasma cleaning), the surface chemistry used (silanization or no silanization), the advancing water contact angle of the surface,
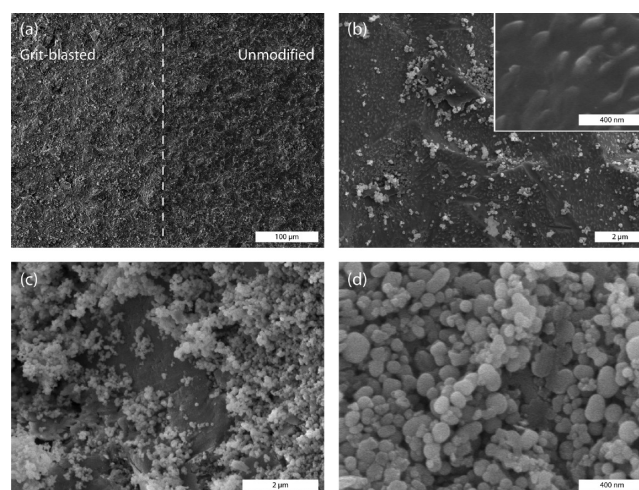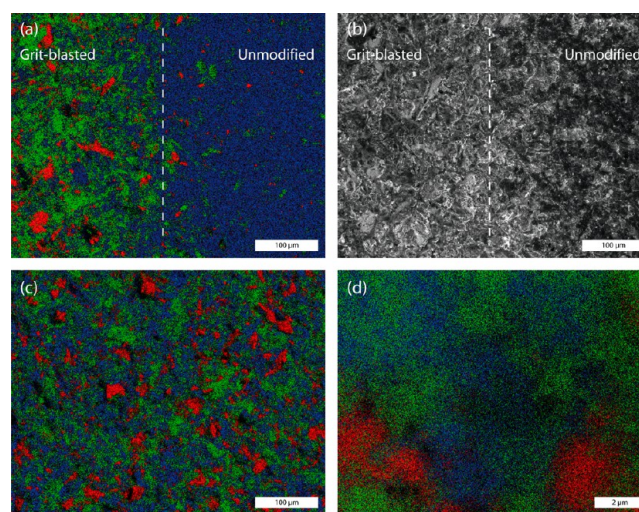
and the result of hydrogel grafting after overnight immersion in deionized water.

Reaction of 3-(trimethoxysilyl)propyl methacrylate to a hydrophilic surface leads to an increase in the water contact angle. As a control, we plasma-cleaned glass and measured the contact angle of surfaces without further treatment and surfaces with silane functionalization, finding that, as expected, contact angles for these are 5° and 63°, respectively.

**Table 1. Measured Parameters for Untreated and SiO₂-Modified Titanium Substrates as well as Untreated Glass**

|  | initial treatment | roughness (nm) | post-treatment | surface chemistry | contact angle (deg) | PEG(1000) graft |
|---|---|---|---|---|---|---|
| titanium | SiO$_2$ grit-blasting | 1708 ± 254 | none | TMSPM[b] | 14 ± 2 | strongly bonded |
|  | SiO$_2$ grit-blasting |  | none | none | 7 ± 2 | delaminated |
|  | SiO$_2$ PECVD[a] | 522 ± 28 | plasma | TMSPM[b] | 53 ± 4 | delaminated |
|  | SiO$_2$ PECVD[a] |  | plasma | none | 2 ± 1 |  |
|  | none | 561 ± 14 | plasma | TMSPM[b] | 82 ± 2 | delaminated |
|  | none |  | plasma | none | 2 ± 1 | delaminated |
|  | none |  | none | TMSPM[b] | 99 ± 2 | delaminated |
|  | none |  | none | none | 98 ± 6 |  |
| glass | none | 7 ± 2 | plasma | TMSPM[b] | 64 ± 3 | delaminated |
|  | none |  | plasma | none | 5 ± 1 |  |

[a]PECVD = plasma enhanced chemical vapor deposition. [b]TMSPM = 3-(trimethoxysilyl)propyl methacrylate.

Before silane-coupling, the grit-blasted samples had a contact angle of 7°. After silane functionalization, the contact angle increased to 14°. In general, the unroughened substrates showed a more dramatic change in hydrophilicity. For instance, the contact angle of the plasma-cleaned PECVD SiO₂-coated titanium increased from 2° to 53° after silanization. An even more pronounced effect was shown on the plasma-cleaned, plain titanium, where the contact angle increased from 2° to 82° after silanization. Untreated titanium (without plasma cleaning) is already relatively hydrophobic, and there was no change in contact angle with silane coupling. Thus, in each case (with the exception of the untreated titanium), there was a change in the water contact angle after silanization, suggesting that the silane coupling reactions were successful on the substrate surfaces. The relatively small change in the contact angle between unsilanized and silanized grit-blasted titanium is presumed to be due to the measured contact angle being dominated by the high surface roughness, where increased surface roughness results in a decrease in measured contact angle.[36]

**Hydrogel Bonding.** PEG(1000)-DMA was cured over the surfaces of all of the silane functionalized surfaces listed in Table 1, with the exception of untreated titanium. The samples were left in deionized water overnight to allow the hydrogel to achieve equilibrium swelling. At the precursor concentration of PEG(1000)-DMA used, the resultant hydrogel swells up to 10% in volume. This isotropic expansion of the hydrogel network is expected to generate stresses at the interface between the hydrogel and underlying substrate to which it is grafted. Therefore, if the bond strength between the hydrogel and the substrate is sufficiently high, then the hydrogel would be expected to remain bonded to the surface even after equilibrium swelling. On the other hand, if the bond strength is low, then the hydrogel would delaminate from the surface due to bond breakage within the network itself near the grafting sites. Of all the cases studied, only the grit-blasted surfaces were successful in retaining the hydrogel after swelling to equilibrium. An example of a successful hydrogel-metal assembly created by the grit-blasting process is shown in Figure 7. The water-swollen hydrogel in the photograph is bonded to the titanium on one side by covalent linkages to an intervening layer of grit-blasted SiO₂. The adhesion strength of the hydrogel-grafted, grit-blasted surfaces was subsequently evaluated by lap-shear adhesion tests.

**Strength of Hydrogel Bonding to Titanium.** The strength of the hydrogel-titanium bonding was tested using lap-shear adhesion experiments in which two titanium plates were adhered together using a 250 μm layer of hydrogel and
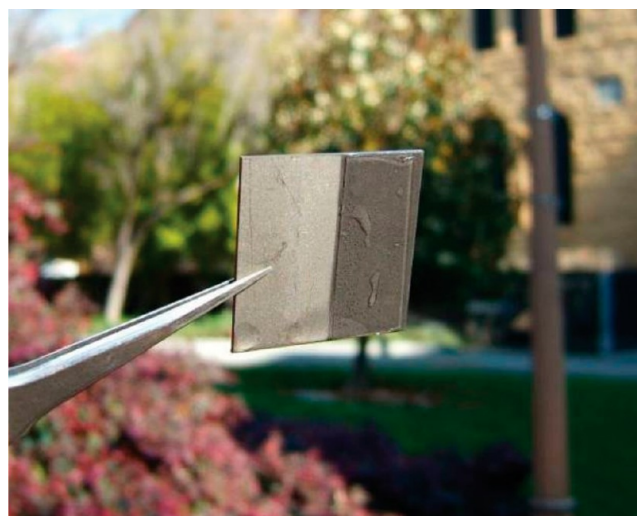


**Figure 7.** Photograph of a hydrogel-titanium assembly made by the tribochemical, grit-blasting grafting process. The hydrogel is bonded to the right-hand side of the titanium plate by covalent linkage to a chemically modified intervening SiO₂ layer. Area of titanium substrate is 6.5 cm².

pulled apart using a tensile testing apparatus. Adhesion to both surface-modified titanium (via tribochemical silyl-methacrylate linkage) and untreated titanium surfaces (no grit-blasting, plasma, silane, or PECVD SiO₂ surface treatment) was tested. In addition, three different hydrogels were tested: (1) a PEG(1000)-DMA single network, (2) a PHEMA single network, and (3) a PEG/PAA semi-interpenetrating network, all of which would be expected to form bonds with the methacrylate groups on the modified titanium surface. Lap-shear experiments were carried out after soaking in deionized water as described previously, and the data obtained is shown in Figure 8 and in Table 2.

The three types of grafted hydrogels exhibited different bonding strengths, as demonstrated by the differences in the load versus extension curves shown in Figure 8. The PEG(1000)-DMA hydrogel was the strongest of the three, with a failure load of 120 N, failure stress of 600 kPa, and shear modulus of 1200 kPa. Without silanization of the grit-blasted surface, the PEG(1000)-DMA hydrogel did not bind to the titanium and delaminated upon overnight soaking in deionized water and therefore was not used for lap-shear testing. This is likely due to the swelling of the hydrogel, leading to shearing of the hydrogel off of the grit-blasted surface. Similar results were observed for bonding of PHEMA hydrogels to silanized and
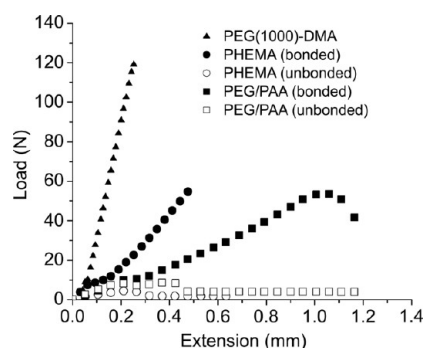
962

dx.doi.org/10.1021/am404361v | ACS Appl. Mater. Interfaces 2014, 6, 958−966

**Figure 8.** Load versus extension data from lap-shear experiments involving PEG-DMA hydrogels (triangles), PHEMA hydrogels (circles), and PEG/PAA semi-IPNs (squares) formed between surface-modified titanium (filled symbols, bonded hydrogels) and untreated titanium (open symbols, unbonded hydrogels).

**Table 2. Degree of Swelling of Hydrogels Used in This Study and Lap-Shear Measured Parameters for Hydrogel Layers Bonded to Surface-Modified Titanium**

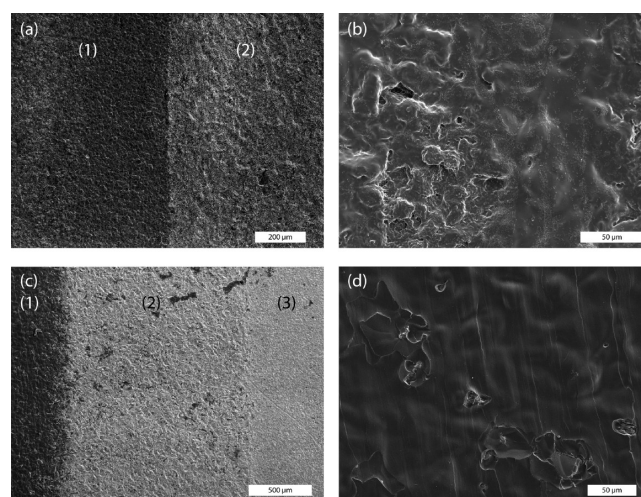|  | degree of swelling (%) | failure load (N) | failure stress (kPa) | shear modulus (kPa) |
|---|---|---|---|---|
| PEG(1000)-DMA | 10 | 120 | 600 | 1200 |
| PHEMA | 35 | 56 | 280 | 300 |
| PEG/PAA | 50 | 53 | 260 | 125 |



**Figure 9.** SEM analysis of PEG(1000) (a, b) and PHEMA (c, d) grit-blasted and silanized samples after lap-shear-induced cohesive failure. (a) Interface between the PEG(1000)-grafted region (1) and the SiO$_2$ modified region (under the Teflon spacer) (2). (b) PEG(1000)-grafted region (within the SiO$_2$ modified area) after lap-shear-induced cohesive failure (i.e., the hydrogel fractured within its bulk). (c) Interface between the PHEMA hydrogel-grafted region (1), grit-blasted region (2), and unmodified region (3). (d) PHEMA-grafted region on SiO$_2$-coated titanium after lap-shear-induced cohesive failure (i.e., the hydrogel fractured within its bulk). Scale bars show (a) 200 $\mu$m, (b, d) 50 $\mu$m, and (c) 500 $\mu$m.

unsilanized grit-blasted titanium (Figure 8, filled and open circles, respectively). The silane-coupled PHEMA hydrogel failed at a load of 56 N, with a failure stress of 280 kPa and shear modulus of 300 kPa. In the case of PHEMA, however, some adhesion was exhibited between the titanium plates without chemical modification (open circles, Figure 8), and thus, a lap-shear experiment could be carried out. This is most likely due to the intrinsically more adhesive or "sticky" surface of the relatively hydrophobic PHEMA hydrogel coupled with the fact that PHEMA exhibits relatively little swelling after polymerization, with a resulting water content of up to 35%. The combination of these factors would facilitate a small level of physical adhesion to the adjacent titanium surface. The load versus extension curves for certain samples also exhibited a buckling region (see PEG/PAA bonded case, extension <0.3 mm) due to the localized detachment of the adhesive at the edges of the sample. In all cases of hydrogel-titanium bond failure, the failure stress is significantly lower than that reported for dental resins adhered to grit-blasted titanium surfaces, where the shear bond strength is reported to be 45 MPa.[35] This indicates that hydrogel-titanium bond failure is not due to delamination of the grit-blasted layer from the titanium surface.

SEM analysis of the PEG(1000) hydrogel-titanium assembly after lap-shear-induced failure (Figure 9a,b) shows a surface morphology significantly different from the grit-blasted titanium surface (Figure 5), suggesting that the surface after lap-shear-induced failure is composed of a polymer film. This evidence, combined with the observation that the thickness of this polymeric layer was on the order of 100 $\mu$m (as measured using SEM relative focal distances), leads to the conclusion that lap-shear-induced cohesive failure took place within the bulk of the hydrogel rather than at the hydrogel-SiO$_2$ interface. SEM analysis of the PHEMA hydrogel-titanium assembly after lap-

shear testing (Figure 9c,d) showed a similar result as for PEG(1000) gels.

In the case of the PEG/PAA semi-IPN bonded to titanium, 53 N of load was required to separate the titanium plates (solid squares, Figure 8). This hydrogel exhibited a fracture stress of 260 kPa and a shear modulus of approximately 125 kPa. As in the case of the unbonded PHEMA network (open squares, Figure 8), some loading (8.1 N) was necessary to pull apart the titanium plates when the titanium was not chemically functionalized. As in the case of the PHEMA, this is most likely due to the intrinsically sticky surface of the PEG/PAA IPN adhering to the titanium. However, in contrast to the bonded case, which failed at a load of 53 N, the PEG/PAA hydrogel was readily delaminated from the untreated titanium surface. This indicates that the tribochemical silyl-methacrylate surface modification is necessary for strong bonding between the PEG/PAA semi-IPN hydrogel and the titanium surface. Even in the bonded case, the PEG/PAA semi-IPN hydrogel layers are less adherent than the PEG(1000) layers. These lap-shear results are contrary to previous bulk uniaxial tensile tests on interpenetrating networks, where double networks were shown to be significantly stronger than single network hydrogels.[37] In the experiments reported here, the strength of the interface between the hydrogel and the grit-blasted surface was tested under shear, not the strength of the material itself under axial load. The reduced adhesion of the semi-IPN is likely due to swelling of the hydrogel during formation of the interpenetrating network. The hydrogel swelling near the titanium surface creates a shear force at the interface, reducing the load required to fracture the hydrogel. In addition, the IPN is only bonded to the titanium through entanglement with the covalently attached PEG network, as shown in Figure 3, and there are no additional attachments resulting from the addition of the PAA.
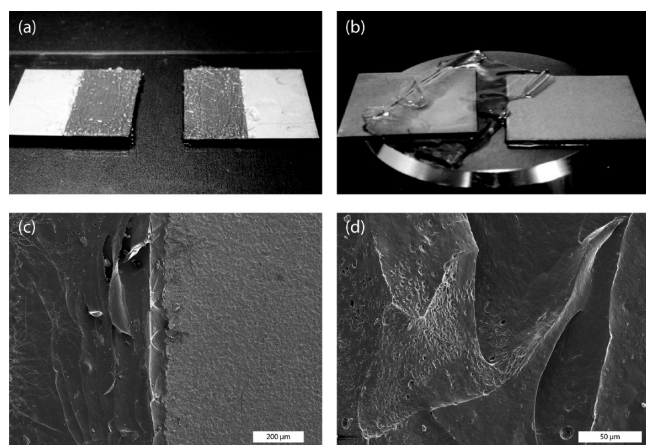
**Figure 10.** Optical micrographs (a, b) and SEM images (c, d) of lap-shear experimental results on titanium plates between which an intervening PEG/PAA semi-IPN was polymerized. (a) Grit-blasted and surface functionalized titanium plates which had been bonded by the hydrogel layer. The rough darkened regions on the plates are the areas that were surface-functionalized and bonded to the hydrogel. The rough appearance is due to the fractured hydrogel material, indicating that the hydrogel bulk failed before the titanium-hydrogel bonds. (b) Appearance of untreated (neither grit-blasted nor chemically modified) titanium. The hydrogel was not bonded to the plates, and as a result, there was no adhesion between the plates. The plates and the hydrogels were easily separated into three parts. (c) SEM showing the PEG/PAA semi-IPN-grafted region on $SiO_2$-coated titanium (left) and the unmodified region (right), after lap-shear-induced cohesive failure. (d) Higher magnification SEM of cohesive hydrogel bulk failure area from (c, left). Plates (a, b) have an area of 6.5 $cm^2$. Scale bars (c, d) show 200 and 50 $\mu$m, respectively.

Gross inspection of the separated titanium samples (Figure 10a,b) showed a stark difference between the chemically bonded and unbonded titanium-hydrogel-titanium "sand-wiches". The chemically bonded samples were separated by fracture of the bulk hydrogel, indicated by the hydrogel material left behind on both sides of the titanium sandwich (Figure 10a). In contrast, the untreated titanium-hydrogel-titanium sandwiches were delaminated along the titanium-hydrogel interface (Figure 10b). The lack of bonding between the hydrogel and the titanium, coupled with the swelling of the hydrogel, led to virtually no adhesion between the materials and ultimate separation into three discrete components (two titanium plates and one hydrogel sheet). SEM analysis (Figure 10c,d) indicates that the failure in the chemically bonded hydrogel occurred primarily within the bulk of the hydrogel rather than at the hydrogel-$SiO_2$ interface, as a layer of hydrogel is still present on the surface of the titanium.

## ■ DISCUSSION

The results from these experiments indicate that both chemical and physical modifications are required for successful grafting of highly swellable hydrogels to titanium surfaces. This effect was also seen in the different surfaces used to bond the PEG-DMA hydrogels (Table 1). Of the various silanized surfaces evaluated, only the grit-blasted titanium was able to retain grafting of the PEG(1000)-DMA hydrogels; all of the unroughened silane-coupled surfaces spontaneously failed in water due to swelling of the PEG(1000)-DMA network after polymerization. The grit-blasted surfaces were three times rougher than the plain titanium and nearly 100 times rougher

than glass. Therefore, roughening of the underlying surface greatly increases the strength of the hydrogel graft, most likely due to a great increase in the surface area for chemical adhesion.

While silane coupling agents enable covalent linkages between certain oxide-containing substrates and polymers, in the case of hydrogel materials with internal osmotic stresses, shear stresses at the bond interface make maintenance of adhesion problematic. We have shown that a flat $SiO_2$ layer deposited via PECVD is not sufficient for achieving robust adhesion between hydrogels and titanium and that a $SiO_2$ coating with higher roughness, for example that produced by $SiO_2$-coated alumina particle grit-blasting, is required for the adhesion process to succeed. This is not unlike what is seen with the bonding of paint primers to natural or synthetic surfaces, where roughening with sandpaper greatly increases the surface area and subsequent adhesion of the primer prior to applying a paint coat. In addition, the island nature of the grit-blasted titanium surface may contribute to increased hydrogel adhesion. The island-based morphology will have a greater average peak to valley (RzDIN) value and, therefore, an increased interlocking component for mechanical adhesion with the hydrogel layer.

We found that the grit-blasting process may not be as chemically homogeneous as specified by the manufacturer of the Rocatec Jr. System. The EDX composition mapping data shows that the grit-blasted surfaces contained roughly equal distributions of $SiO_2$, $Al_2O_3$, and titanium. Neither the chemical homogeneity nor the island nature of the surface, however, necessarily affect the silanization process in a negative manner. It has been reported in the literature that binding of molecules with silane functional groups has also been achieved on $Al_2O_3$,[38,39] and on the native oxide formed on titanium.[40,41] Silane coupling to inorganics such as $SiO_2$, $Al_2O_3$, and $TiO_2$ occurs by a four step mechanism via silanol intermediates.[42] Therefore, despite the fact that $SiO_2$ does not form as a homogeneous coating on the titanium surface, it is likely that a certain degree of silane coupling occurs over the entire grit-blasted surface.

As indicated in Table 1, the PEG(1000)-DMA grafted to the grit-blasted titanium was successfully retained after postpolymerization equilibrium swelling. This means that the gel matrix and/or the chemical bonds with the grit-blasted titanium are strong enough to withstand the small degree of swelling (10 vol %) the network exhibits after polymerization. Similarly, PHEMA networks did not delaminate in the long term, presumably due to lower osmotic pressures inside the gel since the gel does not swell after polymerization. It may also be because of hydrophobic stabilization of the grafted network structure made possible through hydrophobic interaction between the abundant methacrylate groups of PHEMA and the methacrylate groups coupled to the underlying substrate. The PEG/PAA semi-IPN did swell substantially in water (50 vol %) but still remained grafted to the titanium surface. SEM analysis of this material after the lap-shear test showed the presence of polymeric material at the failed interface, indicating that this failure occurred within the bulk of the hydrogel (Figure 10c,d). However, elemental analysis would be useful to ascertain whether the failure is truly within the hydrogel network and not due to failure at the silane coupling level. Unfortunately, X-ray photoelectron spectroscopy and EDX spectroscopy cannot distinguish atoms from the silane coupling agent from those within the hydrogel or on the grit-blasted

surface. Confocal microscopy could potentially be used to obtain further information on the failure mode through the application of a silane coupling agent containing a fluorescent spacer group.

## CONCLUSIONS

Hydrogel-titanium assemblies were created through a grit blasting/silanization process used conventionally in dental applications. Formation of a $SiO_2$ layer on titanium allowed coupling of photoreactive methacrylate groups via silane chemistry and subsequent photoinitiated grafting of methacrylate and acrylate-based hydrogel polymers to the surface of the titanium. The hydrogel-metal interface was studied through a combination of profilometry, SEM/EDX analyses, contact angle measurement, grafted hydrogel swelling, and lap-shear adhesion tests. Profilometry was carried out to determine the roughness of the various surfaces being evaluated while contact angle measurements were done to confirm surface energy changes after plasma cleaning and silanization. Specifically, the bonding of hydrogels to grit-blasted, $SiO_2$-coated titanium samples was compared with that on titanium coated with $SiO_2$ by chemical vapor deposition, untreated titanium, and glass. The grit-blasted surfaces were found to have three-times higher roughness than unblasted titanium. These roughened surfaces were revealed to contain a heterogeneous combination of $SiO_2$, $Al_2O_3$, and titanium, all of which are potentially reactive to the silyl-methacrylate coupling agent used. For the smoother, unroughened surfaces, plasma cleaning was also performed in an attempt to improve silane coupling and subsequent hydrogel adhesion. However, none of the unroughened surfaces facilitated sustained bonding of hydrogel material to the underlying titanium. Single networks of PEG(1000)-DMA, PHEMA, and PEG/PAA semi-IPNs remained grafted to the grit-blasted hydrogel surfaces in pure water. Of the hydrogel-metal assemblies evaluated, PEG(1000)-DMA bonded to the grit-blasted titanium showed the highest adhesion strength.

The implantation of metallic medical devices forms a crucial and integral part of orthopedic and reconstructive surgery. The use of certain polymeric hydrogel-based coatings extends the implant biocompatibility, while increased adhesion between the metallic surface and the polymer coating improves the longevity of the implant. Through the application of the three-stage surface modification procedure outlined in this paper, it is possible to modify a titanium surface with a strongly adherent biocompatible polymeric coating. It is highly likely that this facile process is scalable in terms of modified surface area and should also be applicable to nonplanar surfaces. Since the grit-blasting process is localized and directional, it could provide a route toward implants with hydrogel coatings in discrete and precisely defined areas. This three-stage process could easily be applied to other medically important metals and alloys, such as magnesium alloys.[43,44] In addition, through the use of appropriate surface functionalization and hydrogel chemistries, the process could be used for the adhesion of different hydrogel-based materials, such as smart gels,[45] hydrogels that promote wound healing,[46] and hydrogels that allow drug delivery[1] or act as tissue scaffolds.[47]

## AUTHOR INFORMATION

**Corresponding Author**
*Tel: +1 650 723 4573. Fax: +1 650 723 9780. E-mail: curt. frank@stanford.edu.

**Present Addresses**
†Department of Physics, Imperial College London, Prince Consort Road, London SW7 2AZ, UK.
‖Austrian Institute of Technology, Donau-City-Straße 1, 1220 Vienna, Austria.

**Author Contributions**
‡B.V.O.M. and D.M. contributed equally.

**Notes**
The authors declare no competing financial interest.

## ACKNOWLEDGMENTS

## REFERENCES

(1) Pitarresia, G.; Palumboa, F. S.; Calascibettaa, F.; Fioricaa, C.; Di Stefanoa, M.; Giammona, G. Int. J. Pharm. 2013, 449, 84−94.
(2) Jagur-Grodzinski, J. Polym. Adv. Technol. 2010, 21, 27−47.
(3) Hildebrand, H. F.; Blanchemain, N.; Mayer, G.; Chai, F.; Lefebvre, M.; Boschin, F. Surf. Coat. Technol. 2006, 200, 6318−6324.
(4) Kim, B. S.; Hrkach, J. S.; Langer, R. Biomaterials 2000, 21, 259−265.
(5) Geetha, M.; Singh, A. K.; Asokamani, R.; Gogia, A. K. Prog. Mater. Sci. 2009, 54, 397−425.
(6) Liu, X.; Chu, P. K.; Ding, C. Mater. Sci. Eng., R 2004, 47, 49−121.
(7) Schuler, M.; Trentin, D.; Textor, M.; Tosatti, S. G. P. Nanomedicine 2006, 1, 449−463.
(8) Hanawa, T. J. Periodontal Implant Sci. 2011, 41, 263−272.
(9) Rosca, M.; Vasilescu, E.; Drob, P.; Vasilescu, C.; Drob, S. I. Mater. Corros. 2012, 63, 527−533.
(10) Kim, H.-M.; Miyaji, F.; Kokubo, T.; Nakamura, T. J. Biomed. Mater. Res. 1996, 32, 409−417.
(11) Yamada, M.; Miyauchi, T.; Yamamoto, A.; Iwasa, F.; Takeuchi, M.; Anpo, M.; Sakurai, K.; Baba, K.; Ogawa, T. Acta Biomater. 2010, 6, 4578−4588.
(12) Iwasa, F.; Hori, N.; Ueno, T.; Minamikawa, H.; Yamada, M.; Ogawa, T. Biomaterials 2010, 31, 2717−2727.
(13) Aita, H.; Hori, N.; Takeuchi, M.; Suzuki, T.; Yamada, M.; Anpo, M.; Ogawa, T. Biomaterials 2009, 30, 1015−1025.
(14) Gomez-Vega, J. M.; Saiz, E.; Tomsia, A. P. J. Biomed. Mater. Res. 1999, 46, 549−559.
(15) Grill, A. Diamond Relat. Mater. 2003, 12, 166−170.
(16) Wen, C. E.; Xu, W.; Hu, W. Y.; Hodgson, P. D. Acta Biomater. 2007, 3, 403−410.
(17) Martin, H. J.; Schulz, K. H.; Bumgardner, J. D.; Schneider, J. A. Thin Solid Films 2008, 516, 6277−6286.
(18) De Giglio, E.; Cometa, S.; Ricci, M. A.; Zizzi, A.; Cafagna, D.; Manzotti, S.; Sabbatini, L.; Mattioli-Belmonte, M. Acta Biomater. 2010, 6, 282−290.
(19) De Giglio, E.; Cometa, S.; Ricci, M. A.; Cafagna, D.; Savino, A. M.; Sabbatini, L.; Orciani, M.; Ceci, E.; Novello, L.; Tantillo, G. M.; Mattioli-Belmonte, M. Acta Biomater. 2011, 7, 882−891.
(20) Choi, J.; Konno, T.; Matsuno, R.; Takai, M.; Ishihara, K. Colloids Surf., B 2008, 67, 216−223.
(21) Tan, G.; Zhou, L.; Ning, C.; Tan, Y.; Ni, G.; Liao, Y.; Yu, P.; Chen, X. Appl. Surf. Sci. 2013, 279, 293−299.
(22) Murata, H.; Chang, B.-J.; Prucker, O.; Dahm, M.; Rühe, J. Surf. Sci. 2004, 570, 111−118.

(23) Chang, B.-J.; Prucker, O.; Groh, E.; Wallrath, A.; Dahm, M.; Rühe, J. *Colloids Surf., A* **2002**, *198−200*, 519−526.

(24) Raghuraman, G. K.; Dhamodharan, R.; Prucker, O.; Rühe, J. *Macromolecules* **2008**, *41*, 873−878.

(25) Ibrahim, K. A.; Al-Muhtaseb, A. H.; Prucker, O.; Rühe, J. *J. Polym. Res.* **2013**, *20*, 124−133.

(26) Navarro, R.; Perrino, M. P.; Prucker, O.; Rühe, J. *Langmuir* **2013**, *29*, 10932−10939.

(27) Schuh, K.; Prucker, O.; Rühe, J. *Macromolecules* **2008**, *41*, 9284−9289.

(28) Matinlinna, J. P.; Lassila, L. V. J.; Kangasniemi, I.; Vallitlu, P. K. *J. Dent. Res.* **2005**, *84*, 360−364.

(29) Lung, C. Y. K.; Matinlinna, J. P. *Dent. Mater.* **2012**, *28*, 467−477.

(30) Myung, D.; Muir, B. V. O.; Frank, C. W. Hydrogel-metal assembly. U.S. Patent 8,334,044 B2, December 18, 2012.

(31) Wennerberg, A.; Albrektsson, T.; Johansson, C.; Andersson, B. *Biomaterials* **1996**, *17*, 15−22.

(32) Buser, D.; Nydegger, T.; Oxland, T.; Cochran, D. L.; Schenk, R. K.; Kirt, H. P.; Snétivy, D.; Nolte, L.-P. *J. Biomed. Mater. Res.* **1999**, *45*, 75−83.

(33) Baleani, M.; Viceconti, M.; Toni, A. *Artif. Organs* **2000**, *24*, 296−299.

(34) Lung, C. Y. K.; Matinlinna, J. P. *Dent. Mater.* **2012**, *28*, 467−477.

(35) 3M ESPE Dental Supplies: Rocatec Bonding Scientific Product Profile. http://www.3m.com/intl/kr/medi/medi5/pdf/Rocatec.pdf (accessed Aug 2, 2013).

(36) Wenzel, R. N. *Ind. Eng. Chem.* **1936**, *28*, 988−994.

(37) Myung, D.; Koh, W.; Ko, J.; Hu, Y.; Carrasco, M.; Noolandi, J.; Ta, C. N.; Frank, C. W. *Polymer* **2007**, *48*, 5376−5387.

(38) Abboud, M.; Turner, M.; Duguet, E.; Fontanille, M. *J. Mater. Chem.* **1997**, *7*, 1527−1532.

(39) Kurth, D. G.; Bein, T. *Langmuir* **1995**, *11*, 3061−3067.

(40) Xiao, S. J.; Textor, M.; Spencer, N. D. *Langmuir* **1998**, *14*, 5507−5516.

(41) Nanci, A.; Wuest, J. D.; Peru, L.; Brunet, P.; Sharma, V.; Zalzal, S.; McKee, M. D. *J. Biomed. Mater. Res.* **1997**, *40*, 324−335.

(42) Pluedemann, E. P. In *Silane coupling agents*; Plenum Press: New York, 1982; Chapter 5, pp 116−128.

(43) Wong, H. M.; Yeung, K. W. K.; Lam, K. O.; Tam, V.; Chu, P. K.; Luk, K. D. K.; Cheung, K. M. C. *Biomaterials* **2010**, *31*, 2084−2096.

(44) Hornberger, H.; Virtanen, S.; Boccaccini, A. R. *Acta Biomater.* **2012**, *8*, 2442−2455.

(45) Chaterji, S.; Kwon, I. K.; Park, K. *Prog. Polym. Sci.* **2007**, *32*, 1083−1122.

(46) Myung, D.; Farooqui, N.; Zheng, L. L.; Koh, W.; Gupta, S.; Bakri, A.; Noolandi, J.; Cochran, J. R.; Frank, C. W.; Ta, C. N. *J. Biomed. Mater. Res., Part A* **2009**, *90*, 70−81.

(47) Hoffman, A. S. *Adv. Drug Delivery Rev.* **2012**, *64*, 18−23.